# MOLECULAR DYNAMIC SIMULATION OF GLASS FORMATION AND CRYSTALLIZATION IN BINARY METALLIC ALLOYS DURING COOLING PROCESS

**Sedat SENGUL and Unal DOMEKELI**
*Dept. of Physics, Faculty of Science, Trakya University, Edirne, 22030, Turkey*

**Abstract**

*The rapid solidification of the binary metallic alloy has been studied with the constant-pressure and constant-temperature molecular dynamics technique to obtain an atomistic description of glass formation and crystallization in the alloy. Molecular dynamics simulations have performed through the DL_POLY open source code using on the embedded atom method, which is generally preferred for metallic systems to identify atomic interactions in the system. The effects of different cooling rates on the glass formation and crystallization of binary alloy have studied. The local atomic ordered structures of liquid, glass and crystalline have been characterized by the pair analysis technique. The calculated pair distribution functions during cooling process provided a good picture of the structural transformations, and the results are consistent with results of experimental and ab initio molecular dynamics works in the literature. This consistency indicates that the molecular dynamic results obtained in our study provide a powerful approach to obtain detailed chemical and topological ordering of metallic glasses, liquids and crystalline.*

**Keywords:**Molecular Dynamic Simulations, Rapid Solidification, Pair Analysis Technique, Metallic Glasses, Pair Distribution Function, Pair Analysis Technique

## INTRODUCTION

Understanding of the structural and physical properties of liquid metals is an important step in the processing of amorphous materials and of great technological importance to design functional materials such as metallic glasses (MGs)[1] or to investigate liquid-solid phase[2]. Besides this,due to the technical limitations of the experimental setup, the precise determination of the structural and chemical properties of metallic systems is exhausting and sometimes even impossible. However, a database limited to a single property or even a missing experimental data set can usually be sufficient to perform molecular dynamic (MD) simulations[3]. Recent literature reports have proven that MD simulations are sufficient, and then these simulations have been widely used for the study of the structures, dynamics and thermodynamics of liquid and solid bulk materials[3–9]. Recently, many semi-empirical potentials have been proposed to improve the reliability of classical MD simulations and to better describe the atomic interactions in the system, these potentials can be listed as follows, embedded atomic model (EAM)[10], modified embedded atomic model (MEAM)[11], tight binding (TB)[12] and quantum Sutton-Chen (Q-SC)[13] many-body potential.

The goals of this work is to investigate the effects of the cooling rate on structure evolution of Al-based metal melts ($Al_{60}Cu_{40}$) through classical molecular dynamics simulation by using embedded atom method (EAM). Why did we choose the Al-Cu alloy? Aluminum alloys; they have very heterogeneous microstructures compared to many other metal alloys, they can form alloy with different elements such as zinc, magnesium, silicon, copper and lithium, they have many applications, they are highly resistant to heat treatment, they are good conductors for heat and electricity, and they have high resistance to corrosion.

## EXPOSITION

In our study, we used the EAM potential proposed by Daw and Baskes[10]for the first time to describe the interactions between the Al and Cu atoms in the $Al_{60}Cu_{40}$ system.

Within the EAM formalism, the total energy of a system is formulated as:

$$E_{tot} = \sum_i F_i(\rho_{h,i}) + \frac{1}{2}\sum_{i \neq i} \varphi_{ij}(r_{ij}) \quad (1)$$

$$\rho_{h,i} = \sum_{j \neq i} \rho_{ij}^{a}(r_{ij}) \quad (2)$$

The EAM potential data generated by Howard Sheng was taken from the "https://sites.google.com/site/eampotentials/Home/AlCu" website. In order to identify atomic interactions in the simulation, we preferred the EAM potential, which was previously reported to be successful for metallic systems[14–17], and we realized the simulations with the DL_POLY 2.0 simulation package program[18].For $Al_{60}Cu_{40}$ alloy with 6750 atoms (4050 Al atoms and 2700 Cu atoms), periodic boundary conditions were applied in all three directions. The initial temperature was set at 1400K, which is far above melting point ($T_m$~933K) of $Al_{60}Cu_{40}$alloy. The Nóse Hoover[19] thermostat was used to keep the temperature under control. The system was cooled with different cooling rates (γ=5 K/ps, γ=0.5 K/ps and γ=0.05 K/ps) from 1400 K to 200 K with an intervals of 50 K.

We used energy and volume curves for temperature-dependent changes of the glass transition and crystallization processes. Figure 1 shows the change in the total energy obtained with different cooling rates as a function of temperature. As can be seen from the figure, the total energy curves obtained for all cooling rates are almost linearly reduced between 1400 K and 550 K. At lower temperatures, the energy curves for the γ=5 K/psand γ= 0.5 K/pscooling rates show a slight slope difference and continue to decrease almost linearly. In this temperature range, where the slope difference occurs, it is thought that the system transitioned from liquid to amorphous structure. The intersection points of the linear fit lines drawn to the energy curves in the low and high temperature ranges have been taken as the glass transition temperature ($T_g$) of the system. The $T_g$'s determined at the end of this process are approximately 434 K for γ=5 K/psand about 390 K for γ= 0.5 K/ps, and the $T_g$ calculated for γ= 0.5 K/ps is shown in Figure 1. In our simulation, we observed a systematic relationship between cooling rate and $T_g$. In other words, we observed a decrease in $T_g$'s with decreasing cooling rate. When the system is cooled with a cooling rate of γ=0.05 K/ps, there is a sudden break in the energy curve at low temperatures, unlike other cooling rates. This case shows that if enough time is given to the system, the crystal nucleation continues to increase and finally the system is transitioned from liquid to solid state.

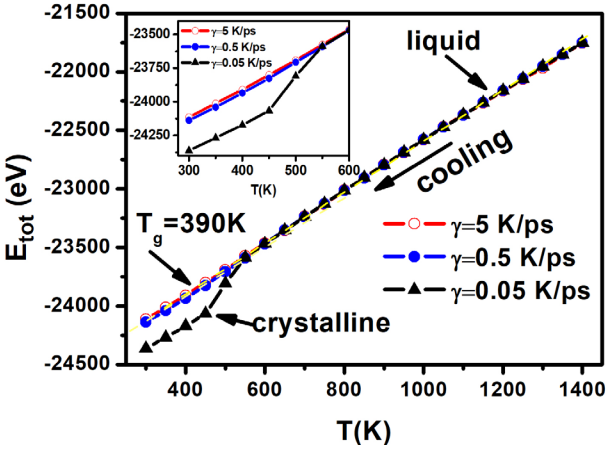


***Fig. 1.*** *Total energy as a function of temperature for $Al_{60}Cu_{40}$ alloy calculated with EAM potential*

We used the pair distribution function (PDF) g(r) to define the structural characterization of the system cooled by different cooling rates [20,21]. It is defined as;

$$g_{i,j}(r) = \frac{L^3}{N_i N_j}\left\langle \frac{\sum_{\alpha=1}^{N_i} n_{\alpha j}(r)}{4\pi r^2 \Delta r} \right\rangle \quad (3)$$

The PDF curves obtained with the cooling rate of γ=0.5 K/ps for the $Al_{60}Cu_{40}$ alloy examined in this study were plotted in Figure 2 and compared with the experimental data measured by Wang et al.[22]. Our results are in good agreement with the experimental results. As expected from the cooled systems, it can be clearly seen that the first peaks of g(r)'s are sharper and higher with the decrease of temperature. This is an indication that the short range order (SRO) of the system increases during the cooling process.

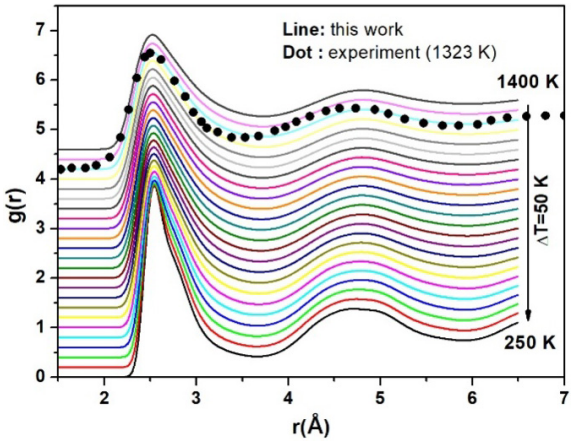


***Fig. 2.*** *Total PDFs of experimental at 1323 K* [22]*and simulated amorphous* $Al_{60}Cu_{40}$ *at different temperatures for cooling rate of γ=0.5 K/ps*

The total PDF curves obtained at 300K for three different cooling rates are shown in Figure 3. The g(r) curves of the system cooled with the cooling rates of γ=5 K/ps and γ=0.5 K/ps are very similar to each other.In order to see the small differences that occur for these cooling rates in a little more detail, we have drawn the first and second peaks of the PDF curves by zooming and we have shown them in the insets of Figure 3. The figure shows that when the system is cooled more slowly, the main peaks of the PDF curves are so high and sharp.In this case, the system is related to the atomic order and SRO. On the other hand, the g (r) curves of the system cooled with a slower cooling rate of γ=0.05 K/ps produce peaks of typical *bcc*crystal-like structures(this case will be discussed in the following sections.). So all the main peaks are much sharper and much more noticeable. These results are consistent with the other analysis results mentioned above.

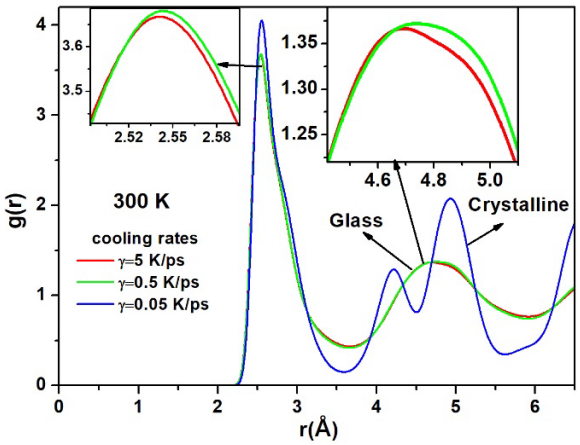


***Fig. 3.*** *Total PDF curves at 300K for* $Al_{60}Cu_{40}$ *alloy cooled using different cooling rates*

In order to get more detailed information about what is going on in adisordered system, we look at the pair analysis where a pair atom and its common neighbors are taken as basic units. We used Honeycutt-Andersen (HA)[23] pair analysis technique, which is an effective technique for filtering the number of different local structures within the simulation system. The number of 1551, 1541 and 1431 bonded pairs *(ICOS types)* in liquid is a direct measurement of the degree of icosahedral order. The 1421 and 1422 bonded pairs *(fcc and hcp types)* and the 1661 and 1441 bonded pairs *(bcc types)* are the characteristic bonded pairs for the *fcc* and *hcp* crystal structure and for the *bcc* crystal structure, respectively. Please see to ref [17,24] for more detailed information. Figure 4 (a) shows that the number of 1551 and 1541 bonded pairs corresponding to an icosahedron cluster at the cooling rate of γ=0.5K/ps increase rapidly as the temperature decreases. With decreasing temperature, the number of bonded pair of 1551 rises to ~25% and occupies a dominant position in the system, indicating that the liquid $Al_{60}Cu_{40}$ receives amorphous condition during the cooling process with a cooling rate of γ=0.5K/ps. Interestingly, the fraction of the 1661 and 1441 bonded pairs, representing the *bcc* crystal structure, is increasing with decreasing temperature. Although there are clusters pointing mostly to amorphous structure in the rapidly solidified system, it is seen that there are also significant clusters in the system indicating different crystalline structures. The results obtained with the γ=5 K/ps cooling rate produce similar results with γ=0.5K/ps and are not shown here to avoid repetition.

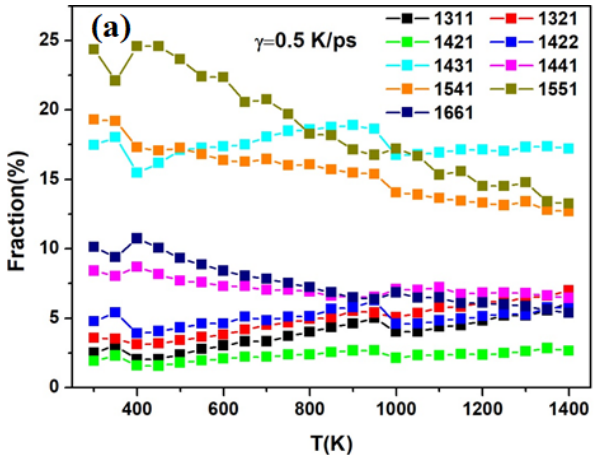

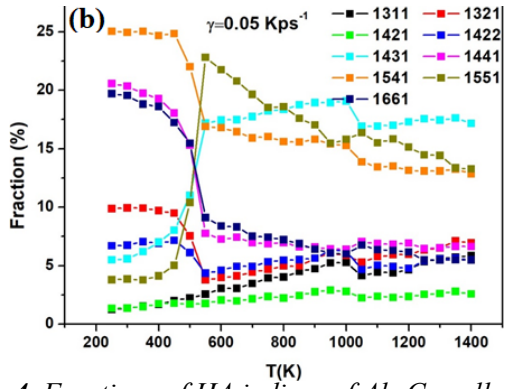


***Fig. 4.*** *Fractions of HA indices of $Al_{60}Cu_{40}$alloy as a functions of temperature: (a) forcooling rate of γ=0.5 K/psand (b) forcooling rate of γ=0.05 K/ps*

Figure 4(b) illustrate the fractions of the HA indices obtained by the cooling rate of γ=0.05 K/ps. In the results obtained from this cooling rate, it clearly shows that *ICOS types* are dominant at high temperatures (between 1400 K and 550 K). However, unlike other cooling rates, the fraction of the 1551 and 1431 bonded pairs have been decreased suddenly at about 550K, while the fraction of the 1541 bonded pairs increased suddenly. This is an interesting case because the 1541 bound pairs are mostly found in amorphous and liquid states and represent the distorted icosahedral ordering. Furthermore, at this temperature, the fraction of the 1441 and 1661 bonded pairs representing the *bcc* crystal structure, the 1321 bonded pairs representing the *rhombohedral* structure, and the 1422 bonded pairs representing the *hcp* crystal structure, are increasing suddenly. These analysis results show that when the system is given enough time, the system transition from liquid structure to crystal structure. The distribution of bcc type clusters at 300K is around ~41%, indicating that the structure tends to be *bcc* crystal, but it is not possible to give accurate information about the structure of the system due to the large amount of other types of clusters.

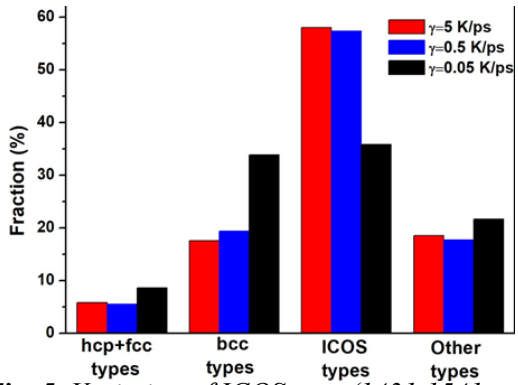


***Fig. 5.*** *Variation of ICOS type (1431,1541 and 1551), fcc and hcp type (1421 and 1422), bcc type (1441 and 1661), and random type (1311, 1321 and others) for different cooling rates at 400 K*

Figure 5 illustrates the distribution of different types of clusters obtained for all cooling rates at 400 K. According to HA analysis, the results obtained using γ=5 K/ps and γ=0.5K /ps cooling rates are very similar. On the other hand, while the distribution of *ICOS* types decreases for the cooling rate of γ=0.05K/ps, the distribution of *bcc* crystal and *other* types increases. These results show that different cooling rates cause significant changes in the system. ICOS-type clusters appear to play an important role for all cooling rates.

## CONCLUSION

In summary, the glass formation and crystallization processes of the $Al_{60}Cu_{40}$ binary alloy cooled using different cooling rates have been investigated with EAM-MD simulations. The calculated PDF results are consistent with the experimental results previously reported in the literature. According to the HA bond-pair analysis, it has been found that a large part of the local structures of the rapidly solidified system for the cooling rates of γ=5 K/ps and γ=0.5 K/pshave been composed of ICOS-type (1551, 1541 and 1431) clusters. It was observed that while the fraction of *ICOS-types* decreased with decreasing cooling rate, especially the fraction of *bcc*-type (1441 and 1661) crystal clusters increased. As a result, it has been observed that when the system is cooled with a cooling rate of γ=0.05 K/ps, liquid-solid phase transition around $T_c$~500 K occurs. These results indicate that the effect of cooling rate causes significant changes in the Al-Cu system.

## REFERENCE

[1] M. Ashby, A. Greer, Metallic glasses as structural materials, Scr. Mater. 54 (2006) 321–326. doi:10.1016/j.scriptamat.2005.09.051.

[2] J.J. Hoyt, M. Asta, Atomistic computation of liquid diffusivity, solid-liquid interfacial free energy, and kinetic coefficient in Au and Ag, Phys. Rev. B. 65 (2002) 214106. doi:10.1103/PhysRevB.65.214106.

[3] M.E. Trybula, P.W. Szafrański, P.A. Korzhavyi, Structure and chemistry of

liquid Al–Cu alloys: molecular dynamics study versus thermodynamics-based modelling, J. Mater. Sci. (2018). doi:10.1007/s10853-018-2116-8.
[4] M. Asta, D. Morgan, J.J. Hoyt, B. Sadigh, J.D. Althoff, D. de Fontaine, S.M. Foiles, Embedded-atom-method study of structural, thermodynamic, and atomic-transport properties of liquid Ni-Al alloys, Phys. Rev. B. 59 (1999) 14271–14281. doi:10.1103/PhysRevB.59.14271.
[5] J. Horbach, S.K. Das, A. Griesche, M.-P. Macht, G. Frohberg, A. Meyer, Self-diffusion and interdiffusion in melts: Al80Ni20 Simulation and experiment, Phys. Rev. B. 75 (2007) 174304. doi:10.1103/PhysRevB.75.174304.
[6] S.K. Das, J. Horbach, M.M. Koza, S. Mavila Chatoth, A. Meyer, Influence of chemical short-range order on atomic diffusion in Al–Ni melts, Appl. Phys. Lett. 86 (2005) 011918. doi:10.1063/1.1845590.
[7] M. Trybula, N. Jakse, W. Gasior, A. Pasturel, Structural and physicochemical properties of liquid Al–Zn alloys: A combined study based on molecular dynamics simulations and the quasi-lattice theory, J. Chem. Phys. 141 (2014) 224504. doi:10.1063/1.4903209.
[8] M.E. Trybula, Structure and transport properties of the liquid Al 80 Cu 20 alloy – A molecular dynamics study, Comput. Mater. Sci. 122 (2016) 341–352. doi:10.1016/j.commatsci.2016.05.029.
[9] M. Celtek, S. Sengul, U. Domekeli, Glass formation and structural properties of Zr50Cu50-xAlxbulk metallic glasses investigated by molecular dynamics simulations, Intermetallics. 84 (2017) 62–73. doi:10.1016/j.intermet.2017.01.001.
[10] M.S. Daw, M.I. Baskes, Embedded atom method: derivation and application to impurities,surfaces and other defects in metal, Phsical Rev. B. 29 (1984) 6443–6453.
[11] B.-J. Lee, M.I. Baskes, Second nearest-neighbor modified embedded-atom-method potential, Phys. Rev. B. 62 (2000) 8564–8567. doi:10.1103/PhysRevB.62.8564.
[12] F. Cleri, V. Rosato, Tight-binding potentials for transition metals and alloys, Phys. Rev. B. 48 (1993) 22–33. doi:10.1103/PhysRevB.48.22.
[13] T. Cagin, Y. Qi, H. Li, Y. Kimura, H. Ikeda, W.L. Johnson, W.A. Goddard, The Quantum Sutton-Chen Many-Body Potential for Properties of fcc Metals, MRS Symp. Ser. 554 (1999) 43.
[14] L. Zhong, J. Wang, H. Sheng, Z. Zhang, S.X. Mao, Formation of monatomic metallic glasses through ultrafast liquid quenching, Nature. 512 (2014) 177. http://dx.doi.org/10.1038/nature13617.
[15] Y.Q. Cheng, H.W. Sheng, E. Ma, Relationship between structure, dynamics, and mechanical properties in metallic glass-forming alloys, Phys. Rev. B - Condens. Matter Mater. Phys. 78 (2008) 1–7. doi:10.1103/PhysRevB.78.014207.
[16] M. Celtek, S. Sengul, U. Domekeli, Glass formation and structural properties of Zr50Cu50-xAlx bulk metallic glasses investigated by molecular dynamics simulations, Intermetallics. 84 (2017) 62–73. doi:10.1016/j.intermet.2017.01.001.
[17] M. Celtek, S. Sengul, Thermodynamic and dynamical properties and structural evolution of binary Zr 80 Pt 20 metallic liquids and glasses: Molecular dynamics simulations, J. Non. Cryst. Solids. 498 (2018) 32–41. doi:10.1016/j.jnoncrysol.2018.06.003.
[18] W. Smith, T.R. Forester, DL_POLY_2.0: A general-purpose parallel molecular dynamics simulation package, J. Mol. Graph. 14 (1996) 136–141. doi:10.1016/S0263-7855(96)00043-4.
[19] S. Nosé, A unified formulation of the constant temperature molecular dynamics methods, J. Chem. Phys. 81 (1984) 511–519. doi:10.1063/1.447334.
[20] M. Celtek, S. Sengul, The characterisation of atomic structure and glass-forming ability of the Zr–Cu–Co metallic glasses studied by molecular dynamics simulations, Philos. Mag. 98 (2018) 783–802. doi:10.1080/14786435.2018.1425012.
[21] S. Sengul, M. Celtek, U. Domekeli, Molecular dynamics simulations of glass formation and atomic structures in Zr60Cu20Fe20 ternary bulk metallic alloy, Vacuum. 136 (2017). doi:10.1016/j.vacuum.2016.11.018.
[22] S.Y. Wang, M.J. Kramer, M. Xu, S. Wu, S.G. Hao, D.J. Sordelet, K.M. Ho, C.Z. Wang, Experimental and ab initio molecular dynamics simulation studies of liquid Al 60 Cu 40 alloy, Phys. Rev. B. 79 (2009) 144205. doi:10.1103/PhysRevB.79.144205.
[23] J.D. Honeycutt, H.C. Andersen, Molecular Dynamics Study of Melting and Freezing of Small Lennard- Jones Clusters, J. Phys. Chem. 91 (1987) 4950–4963. doi:10.1021/j100303a014.
[24] F.A. Celik, Molecular dynamics simulation of polyhedron analysis of Cu–Ag alloy under rapid quenching conditions, Phys. Lett. A. 378 (2014) 2151–2156. doi:http://dx.doi.org/10.1016/j.physleta.2014.05.019.